Water Research 141 (2018) 340–348

Contents lists available at ScienceDirect

Water Research

journal homepage: www.elsevier.com/locate/watres

Morphospecies-dependent disaggregation of colonies of the cyanobacterium *Microcystis* under high turbulent mixing

Ming Li [a, b, *, 1], Man Xiao [c, d, 1], Pei Zhang [e, f], David P. Hamilton [c]

[a] College of Natural Resources and Environment, Northwest A & F University, Yangling 712100, PR China
[b] Collaborative Innovation Center of Water Security for Water Source Region of Mid-line of South-to-North Diversion Project, Nanyang Normal University, Nanyang, 473061, PR China
[c] Australian Rivers Institute, Griffith University, Nathan, QLD 4111, Australia
[d] School of Environment, Griffith University, Nathan, QLD 4111, Australia
[e] State Key Laboratory of Hydrology-Water Resources and Hydraulic Engineering, Hohai University, Nanjing, 210098, PR China
[f] School of Civil Engineering, University of Queensland, St Lucia, QLD 4072, Australia

ARTICLE INFO

Article history:
Received 22 December 2017
Received in revised form
8 May 2018
Accepted 10 May 2018
Available online 11 May 2018

Keywords:
Artificial mixing
Colony formation
Turbulent dissipation rate
Kolmogorov scale
Microcystis
Morphospecies

ABSTRACT

Preventing formation of large colonies and reducing colony size of the cyanobacterium *Microcystis* may lead to reductions in bloom formation. Here we investigated the effects of artificial mixing on morphology and disaggregation dynamics of *Microcystis* colonies in vivo, using a stirring device and a laser particle analyzer. The turbulent dissipation rate (ε) was varied from 0.020 to 0.364 $m^2 s^{-3}$. We hypothesized that colonies of *M. aeruginosa* and *M. ichthyoblabe* would be more susceptible to disaggregation from turbulent mixing than colonies of *M. wesenbergii*. Our results showed that colony size of *M. aeruginosa* and *M. ichthyoblabe* decreased with increased turbulence intensity and duration of stirring for $\varepsilon > 0.094\ m^2 s^{-3}$, while *M. wesenbergii* showed less obvious changes in colony size with mixing. Spherical *M. wesenbergii* colonies exposed to high turbulence intensities for 30 min gradually transitioned to colony morphologies similar to *M. ichthyoblabe* and *M. aeruginosa*-like colonies (irregular, elongated or lobed, with distinct holes). Our results suggest that turbulent mixing is an important factor driving morphological changes of *Microcystis* colonies, and artificial mixing may effectively reduce colony size of *Microcystis*, thereby preventing bloom formation.

1. Introduction

Size and morphology of cyanobacteria, particularly colony formation, critically affect grazing pressure by zooplankton, migration velocities, and nutrient uptake (Xiao et al., 2018). They determine whether populations are entrained into the prevailing mixed layer turbulence or become buoyant, which is often associated with surface bloom formation (Oliver et al., 2012; Wallace et al., 2000).

Microcystis is a genus of cyanobacteria with high phenotypic plasticity. It exists mostly as single cells under laboratory culture conditions (Li et al., 2013; Yang et al., 2008), but can form surface 'scums' consisting of large colonies (100–2000 μm) in the field (Rowe et al., 2016; Zhu et al., 2014). Colony size and morphology determine the vertical floating velocity of *Microcystis* colonies and whether colonies can dis-entrain from turbulent mixing to float up towards the water surface and form blooms (Wallace et al., 2000). The floating velocity is usually described by Stoke's Law, based on density, colony size, and morphology (termed the shape coefficient). These three variables differ widely amongst *Microcystis* morphospecies (Li et al., 2016).

Artificial mixing in the laboratory is highly effective in disaggregating colonies of *Microcystis* but most work has been limited to examining particular morphospecies, i.e., *M. aeruginosa* (O'Brien et al., 2004; Regel et al., 2004). Morphospecies such as *M. wesenbergii*, *M. flos-aquae*, *M. ichthyoblabe* and *M. aeruginosa* may dominate in natural eutrophic systems and often undergo successional sequences in these systems (Jia et al., 2011; Ozawa et al., 2005; Park et al., 1993; Yamamoto and Nakahara, 2009; Zhu et al., 2016). Based on spatial distributions of *Microcystis* morphospecies, Otten and Paerl (2011) deduced that colonies of *M. aeruginosa* and *M. ichthyoblabe* are more susceptible to wind

* Corresponding author. College of Natural Resources and Environment, Northwest A & F University, Yangling 712100, PR China.
E-mail addresses: lileaf@163.com, lileaf@nwsuaf.edu.cn (M. Li).
[1] These authors contributed equally. The authors declare no conflict of interest.

https://doi.org/10.1016/j.watres.2018.05.017
0043-1354/

shear than those of *M. wesenbergii* and *M. flos-aquae*. Disaggregation of *Microcystis* colonies at the morphospecies level, however, has not been systematically investigated or quantified.

Colony morphology of *Microcystis* changes when mucilage surrounding the colonies is dissolved (Li et al., 2014b). The process of mucilage dissolution might also be accelerated by mixing. Thus, the interactions of mixing, colony morphology and physiological status of *Microcystis* are likely to have a key regulatory role in bloom formation. In this study our primary objective was to quantify the effects of turbulent mixing, using artificial stirring, on morphological changes and colony disaggregation of three *Microcystis* morphospecies.

2. Material and methods

2.1. Collection of Microcystis colonies

Microcystis colonies were collected from Meiliang Bay (31°24′–31°28′N, 120°10′–120°12′E) in Lake Taihu, China. This bay is located in the northern part of Lake Taihu where frequent and severe *Microcystis* blooms have occurred over the last two decades (Duan et al., 2009). *Microcystis* colonies were sampled on 2 July, 7 September and 15 October 2014, when three distinct morphospecies could be distinguished: *M. ichthyoblabe*, *M. wesenbergii* and *M. aeruginosa*. Colonies were gently filtered through sieves of different pore sizes into three size groups, representing small, medium and large colonies (Fig. S1). The three size groups corresponded to different colony sizes of *Microcystis* morphospecies: Colonies of *M. ichthyoblabe* were divided into <212, 212–300 and > 300 μm, indicative of small, medium and large sized groups, *M. wesenbergii* into <300, 300–500 and > 500 μm, and *M. aeruginosa* into <500, 500–600 and > 600 μm.

2.2. Experimental setup

The mixing experiment was carried out using a laser particle analyzer (Mastersizer 2000 Particle Size Analyzer, Malvern Instruments, Ltd). The propeller has three blades and was set 15 mm above the bottom of a 500 mL beaker (Fig. 1a). The propeller was connected to the analyzer with a pump to mix the media in the beaker during the experiment (Fig. 1a). The propeller was set at rotation speeds of 600, 800, 1000, 1200, 1400 and 1600 rpm, and run for 30 min at each speed. From preliminary experiments, a rotation speed of 600 rpm was found through trial and error to produce minimal disaggregation of *Microcystis* colonies of all the three morphospecies, and 1600 rpm produced significant disaggregation without visible air bubbles.

For each group of mixing experiments, background measurements were firstly conducted using 450 mL of tap water in the beaker without added *Microcystis* colonies (Fig. 1a). Thereafter, the three size groups of the three *Microcystis* morphospecies were gently mixed into the beaker for measurements of colony size distribution. Measurements started when the obscuration parameter of particle size analyzer, which reflects concentration of colonies in the beaker, reached 15%. Here, the obscuration value of 15% was chosen because it is the optimal concentration for the laser particle analyzer to pick up the size distribution. The values of intrinsic refractive index (n) and absorption of light by the particle (k) by the laser particle analyzer were set to 1.40 and 0.1, based on extensive tests conducted by Li et al. (2014b).

The distribution of colony sizes was measured by laser particle analyzer every 2 min. D_{50} of each sample was used to assess variation in colony size, defined as the diameter where 50% of the total biovolume is below this size. After 30 min of mixing, the treated samples were collected for microscopic observation and compared with samples not subjected to mixing.

2.3. Calculation of turbulent dissipation rates and Kolmogorov scale

A modified Discrete Element Lattice Boltzmann Method (DELBM) was used to simulate mixing intensity during the mixing experiment. DELBM is a relatively new computational fluid dynamics (CFD) method used to delineate fluid structure and fluid-particle interactions (Galindo Torres et al., 2016; Galindo-Torres, 2013; Zhang et al. 2016, 2017). The model has been validated in similar studies of rigid object-fluid interactions (Galindo Torres et al., 2016; Zhang et al., 2016). The main advantage of this model is its ability to efficiently and accurately resolve the momentum exchanges between rigid, irregularly shaped objects and the fluid, without re-meshing (Galindo-Torres, 2013; Galindo-Torres et al., 2012). A Smagorinsky subgrid turbulence module was employed to simulate at high Reynolds numbers, using a Smagorinsky constant set to 0.14 (Galindo-Torres, 2013; Zhang et al., 2016).

For DELBM simulations, the shape of propeller is described by a three-dimensional polygon mesh, where the impeller is resolved using a Computed Tomography (CT) scan to minimize error in the numerical representation of the propeller shape. The original very fine mesh from the CT scan was reduced to a coarser resolution (see Fig. 1b–g) without losing the general shape of the propeller, based on preliminary simulations. Two grid resolutions ($88 \times 88 \times 110$ and $176 \times 176 \times 220$) for the beaker were tested to check the independence of simulations on the grid resolution, i.e., the difference between the two resolutions were found negligible. Thus, the grid resolution and the time step were set to 1×10^{-3} m and 5×10^{-5} s, respectively, and approximately 850,000 lattices were used to represent the beaker in the simulation. The relaxation parameter, which is a dimensionless parameter dependent only on the viscosity, was set to 0.500015 corresponding to the viscosity of water at room temperature during the mixing experiment.

Values of total turbulent kinetic energy (TKE, $m^2\ s^{-2}$), turbulent dissipation rate (ε, $m^2\ s^{-3}$) and Kolmogorov scale (μm) determined from DELBM simulations are given for each mixing speed (Table 1). The calculation of ε depends on the average velocity, which is determined from steady state simulations. Therefore, all simulations at each speed were run to steady state, indicated by the magnitude of the dimensionless velocity, as shown in Fig. 1b–g. Our simulated results of TKE, ε, and Kolmogorov scale were similar to those measured in Xiao et al. (2016), which the stirring device and range of rotation speeds were employed similarly to our study.

2.4. Measurement of colony size and morphospecies

For each mixing experiment, the size and morphospecies of *Microcystis* colonies were analyzed by taking photomicrographs using an Olympus C-5050 digital camera coupled to an Olympus CX31 optical microscope. The photomicrographs were analyzed using the UTHSCSA ImageTool v3.00 software (Department of Dental Diagnostic Science, University of Texas Health Science Center, San Antonio, TX, USA). A minimum of 200 colonies per sample was analyzed to calculate the percentage of biovolume of various morphospecies for each size group of each morphospecies (*M. ichthyoblabe*, *M. aeruginosa* and *M. wesenbergii*). *Microcystis* morphospecies were identified following the taxonomic methods of Yu et al. (2007). Only the classical spherical *M. wesenbergii* colonies were identified as *M. wesenbergii* as shown in Fig. 4e. The irregularly branched spherical colonies with no visible mucilage were considered a transitional morphological form of *M. wesenbergii*. The reticulated colonies with visible margins were categorized as reticular *M. wesenbergii*. The biovolume of individual colonies was calculated assuming they were spherical. This

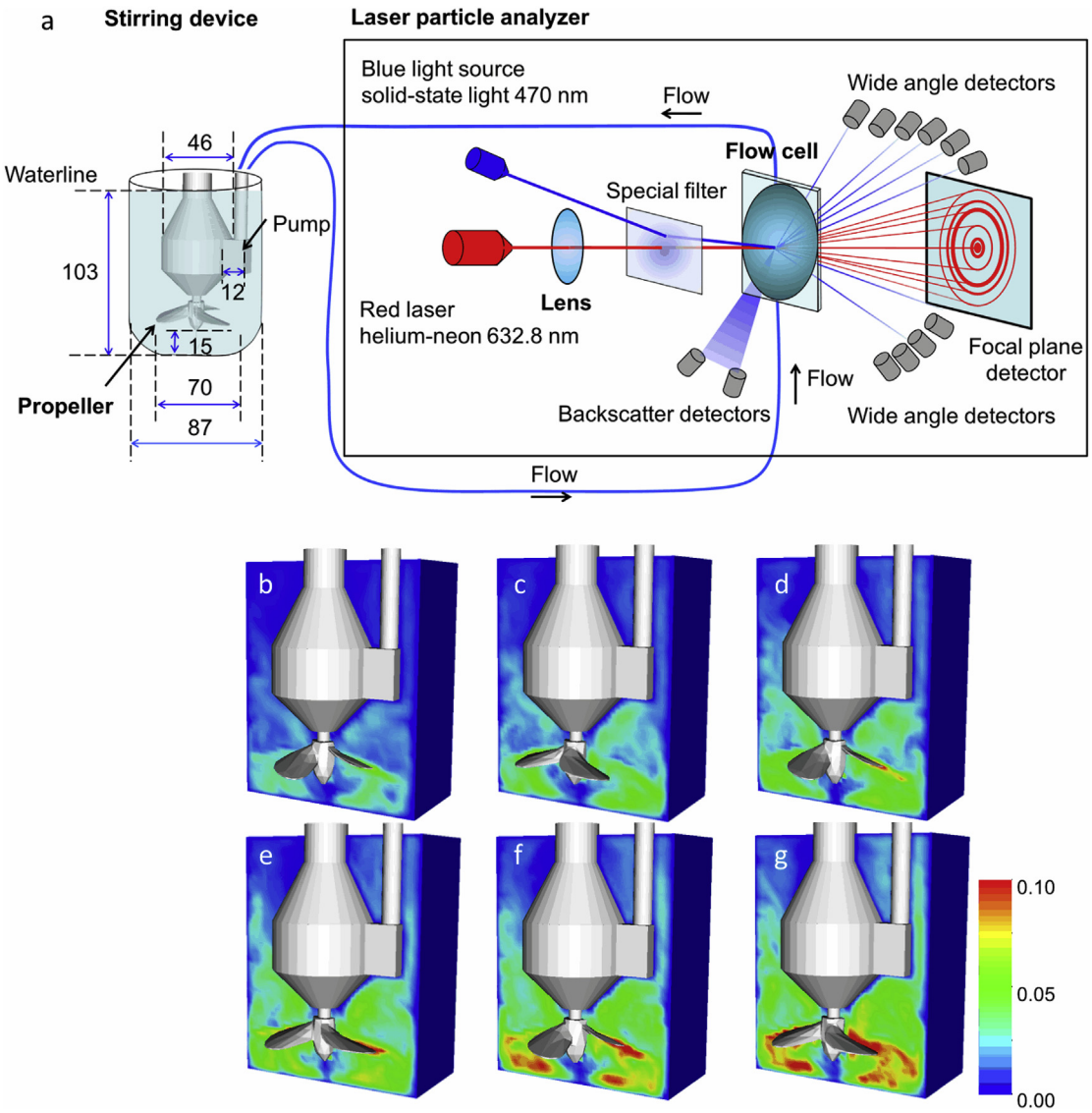

Fig. 1. (a) Schematic of the beaker and propeller used to mix *Microcystis* samples and the laser particle analyzer used to measure colony size distribution. The propeller is described by three-dimensional polygon meshes using a Computed Tomography (CT) scan to minimize numerical shape differences between simulations and the observed set-up. (b–g) Steady-state total turbulent kinetic energy (TKE, $m^2\ s^{-2}$) under the six rotation speeds: a. 600 rpm; b. 800 rpm; c. 1000 rpm; d. 1200 rpm; e. 1400 rpm; and f. 1600 rpm. Units for the stirring device are mm, and color bar from blue to red indicates the magnitude of dimensionless velocity, increasing from 0 to 0.100. (For interpretation of the references to colour in this figure legend, the reader is referred to the Web version of this article.)

approximation was applied because currently there are no reliable methods to accurately measure and calculate the diameter of *Microcystis* colonies, especially those with irregular morphologies. The length and width of colonies were measured directly from the longest axis (length) and the shortest axis (width, aligned perpendicular to the longest axis). The diameter of *Microcystis* colonies was calculated as diameter = $(\text{length} \times \text{width})^{1/2}$ (Li et al., 2014a).

3. Results

3.1. Effects of turbulence on disaggregating Microcystis colonies

The effects of turbulent mixing on disaggregation of *Microcystis* colonies differed substantially, depending on morphospecies, mixing intensity and mixing duration (Fig. 2). *M. ichthyoblabe*, which has tightly packed cells, was most easily disaggregated

Table 1
Turbulent kinetic energy (TKE, $m^2\ s^{-2}$), turbulent dissipation rate ($m^2\ s^{-3}$) and Kolmogorov microscale (μm) at the six rotation speeds, estimated by the computational fluid dynamics (CFD) hydrodynamic model (Discrete Element Lattice Boltzmann Method, DELBM).

Experiment	1	2	3	4	5	6
Speed of the propeller (rpm)	600	800	1000	1200	1400	1600
Turbulent kinetic energy ($m^2\ s^{-2}$)	0.0030	0.0053	0.0083	0.0117	0.0157	0.0206
Turbulent dissipation rate ($m^2\ s^{-3}$)	0.020	0.048	0.094	0.155	0.241	0.364
Kolmogorov microscale (μm)	83.6	67.5	57.1	50.3	45.1	40.7

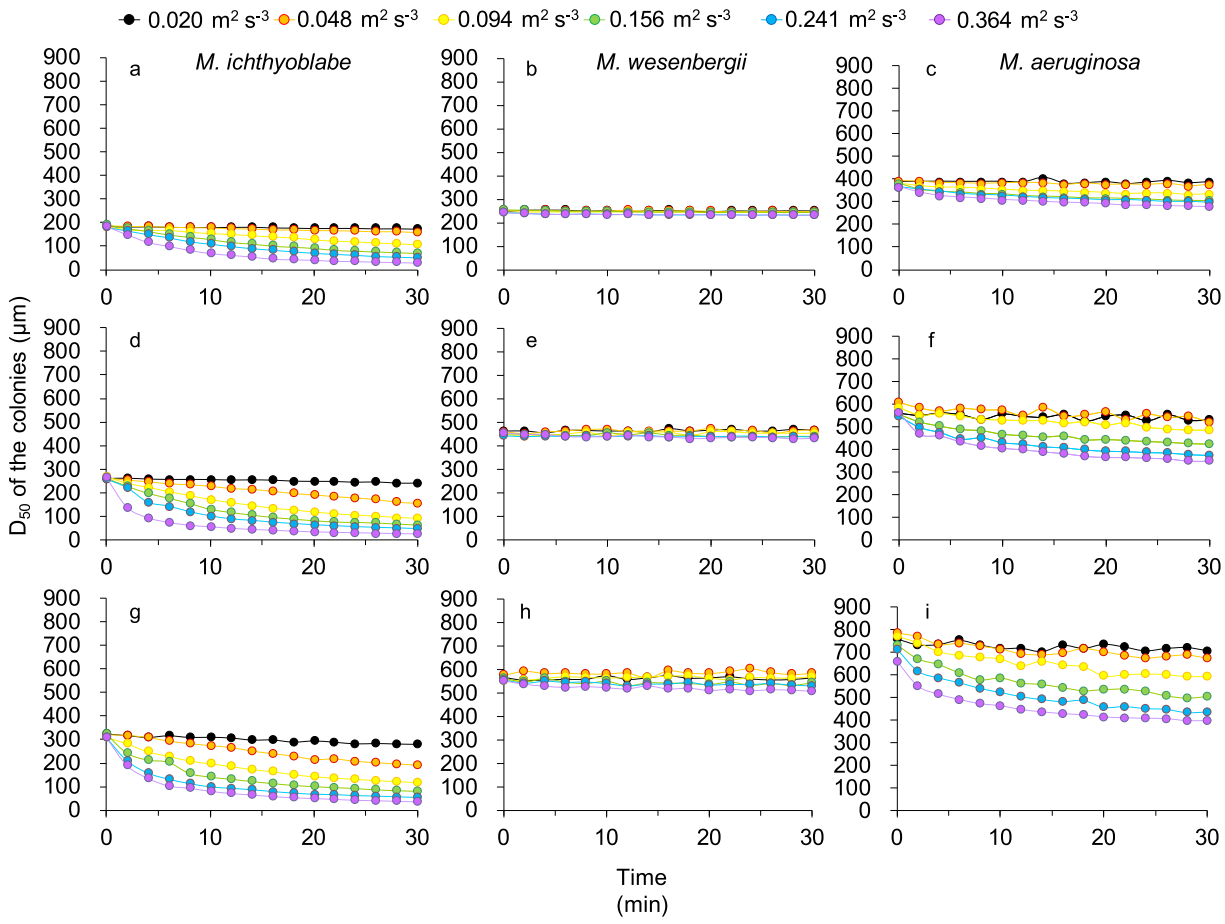

Fig. 2. D_{50} (50% of the population is smaller than this size) of colonies (μm) during the 30-min mixing of the three *Microcystis* morphospecies. a, small *M. ichthyoblabe* colony; b, small *M. wesenbergii* colony; c, small *M. aeruginosa* colony; d, medium *M. ichthyoblabe* colony; e, medium *M. wesenbergii* colony; f, medium *M. aeruginosa* colony; g, large *M. ichthyoblabe* colony; h, large *M. wesenbergii* colony; i, large *M. aeruginosa* colony. Dots in different colours showed the six different rotation speeds. (For interpretation of the references to colour in this figure legend, the reader is referred to the Web version of this article.)

(Fig. 2a, d, g), followed by *M. aeruginosa* (Fig. 2c, f, i) and *M. wesenbergii* (Fig. 2b, e, h). *M. ichthyoblabe* colonies were not affected at the lowest mixing intensity ($\varepsilon = 0.02\ m^2\ s^{-3}$), but the D_{50} (where 50% of the total biovolume is below this size) of the three size groups all decreased sharply to approximately 75% of the initial value after 30-min mixing at ε of $0.094\ m^2\ s^{-3}$ (Fig. S1). At the maximum ε of $0.364\ m^2\ s^{-3}$, D_{50} of *M. ichthyoblabe* colonies from all three size groups decreased to <100 μm after 10-min mixing and to <40 μm after 30-min mixing. In comparison, for ε of $0.094\ m^2\ s^{-3}$ there was little disaggregation of *M. aeruginosa* colonies, which has elongated morphology and distinct holes. The D_{50} decreased to about 75% of the initial value for ε of $0.364\ m^2\ s^{-3}$ after 30-min mixing. Colonies of *M. wesenbergii*, which are spherical and elongated with a visible outer colony margin, barely disaggregated under any of the mixing intensities, irrespective of the initial colony size.

The final colony size of all *Microcystis* morphospecies always decreased with decreasing Kolmogorov scale values calculated from the mixing intensities. Nevertheless, only *M. ichthyoblabe* colonies could be disaggregated to the minimum size after 30-min mixing at a dissipation rate ε of $0.364\ m^{-2}\ s^{-3}$ (Fig. 3a, d, g). In addition, for all the three morphospecies, the large size group was more susceptible to turbulent mixing than the small size group (Fig. 3).

3.2. Changes in colonial morphology induced by turbulence

Colonies of *M. ichthyoblabe*, *M. aeruginosa* and *M. wesenbergii* all underwent morphological changes after 30 min under all six mixing intensities (Fig. 4). *M. ichthyoblabe* colonies changed from a loosely assembled outer mass with tightly packed inner cells (Fig. 4a) to smaller and tightly packed masses (Fig. 4b). *M. aeruginosa* colonies had the least visible morphological changes with mixing, and remained irregular with lobes, distinct holes and irregular shapes (Fig. 4c and d). *M. wesenbergii* colonies transitioned gradually from initially spherical or elongated morphology with visible outer margins which retained mucilage (Fig. 4e) to reticular forms (Fig. 4f), and then to forms with distinct holes and weakly resolved colony margin, similar to those of *M. aeruginosa* (Fig. 4g).

M. wesenbergii colonies transitioned after 30-min mixing to varied proportions of reticular and *M. aeruginosa*-like morphologies, depending on mixing intensities and initial colony sizes (Fig. 5). The incidence of spherical *M. wesenbergii* colonies decreased from about 90% to 55%, 50% and 20% at ε of $0.364\ m^{-2}\ s^{-3}$ for small (Fig. 5a), medium (Fig. 5b) and large (Fig. 5c) size groups, respectively. In comparison, at the lower ε of $0.02\ m^{-2}s^{-3}$, the incidence of spherical *M. wesenbergii* colonies decreased to 80%, 55% and 50% for each of the three size groups.

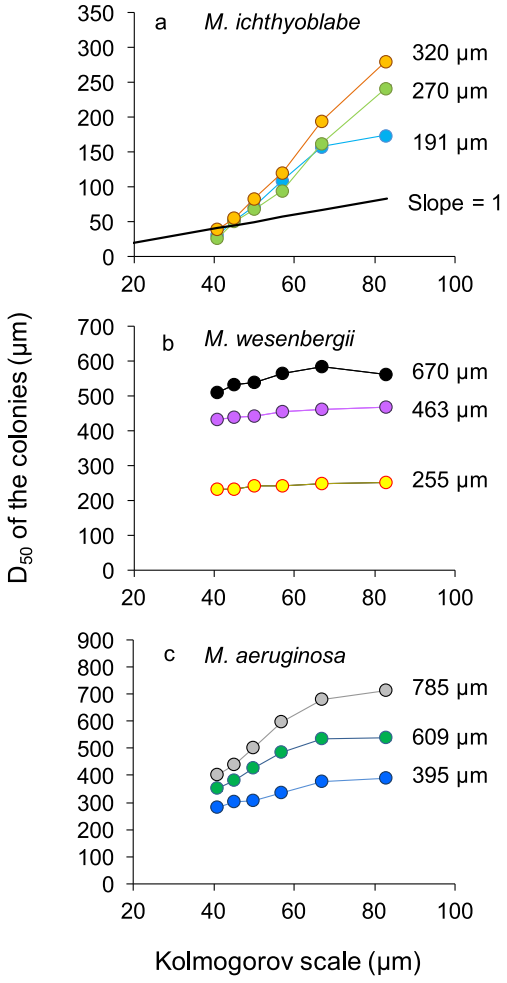

Fig. 3. Relationship between D_{50} of the three size groups of the three *Microcystis* morphospecies after 30-min mixing against the Kolmogorov scale (μm). The Kolmogorov scale was simulated by the DELBM model under the six rotation speeds. a, *M. ichthyoblabe*; b, *M. wesenbergii*; and c, *M. aeruginosa*. The initial D_{50} (μm) values for each sieved size groups were marked for each morphospecies. Slope = 1 corresponds to the minimum size of disaggregated colonies and is similar to the Kolmogorov scale (μm).

4. Discussion

4.1. Turbulent dissipation rate assessment

Our results demonstrate that *M. ichthyoblabe* and *M. aeruginosa* colonies could be potentially disaggregated by high turbulent mixing, while *M. wesenbergii* colonies showed little disaggregation, even at ε approaching five orders of magnitude higher than the highest values measured in deep lakes (10^{-11} – 10^{-6} $m^2 s^{-3}$) (Wüest and Lorke, 2003). The turbulent dissipation rate in Lake Taihu, a large, shallow lake in Jiangsu province, China with a mean depth of 2 m, was reported to range from 6.014×10^{-8} to 2.389×10^{-4} $m^2 s^{-3}$ (Zhou et al., 2016). The maximum value *in situ* was approximately one-tenth of the minimum value employed in the current study. The investigations by Zhou et al. (2016) were conducted in the field using an acoustic Doppler velocimeter, with sampling unable to be conducted on very windy days. MacKenzie and Leggett (1993) described turbulent dissipation rate as a function of wind speed in aquatic environments:

$$\varepsilon = 5.82 \times 10^{-6} w^3 / h \quad (1)$$

where w is wind speed (m s^{-1}) and h is the water depth (m). From this equation, considering the depth of Lake Taihu as 2 m, the wind speed during the field investigation by Zhou et al. (2016) may be in the range 0.275–4.35 m s^{-1}. Measured wind speeds in Lake Taihu can be 5.5–10.7 m s^{-1} for 32.6% of the time and 10.8–17.1 m s^{-1} for 1.22% of time (Wang et al., 2016). Since the turbulent dissipation rate increases with the wind speed, the upper limit of dissipation rate in shallow lakes such as Lake Taihu may be much higher than the reported value of 2.389×10^{-4} $m^2 s^{-3}$. Theoretically, the minimum turbulent dissipation rate used in the current study (0.020 $m^2 s^{-3}$) could almost equate to a wind speed of 19.0 m s^{-1} in Lake Taihu, which was slightly higher than the maximum reported wind speed in Lake Taihu (17.1 m s^{-1}; Wang et al., 2016). In the absence of turbulent dissipation rates recorded at very strong wind speeds, we assumed that the minimum value of turbulent dissipation rate in the current study was similar to that of Lake Taihu under extreme wind conditions, such as a typhoon.

Although artificial mixing by aeration, diffusers or pumping devices has been on occasions used to control cyanobacterial

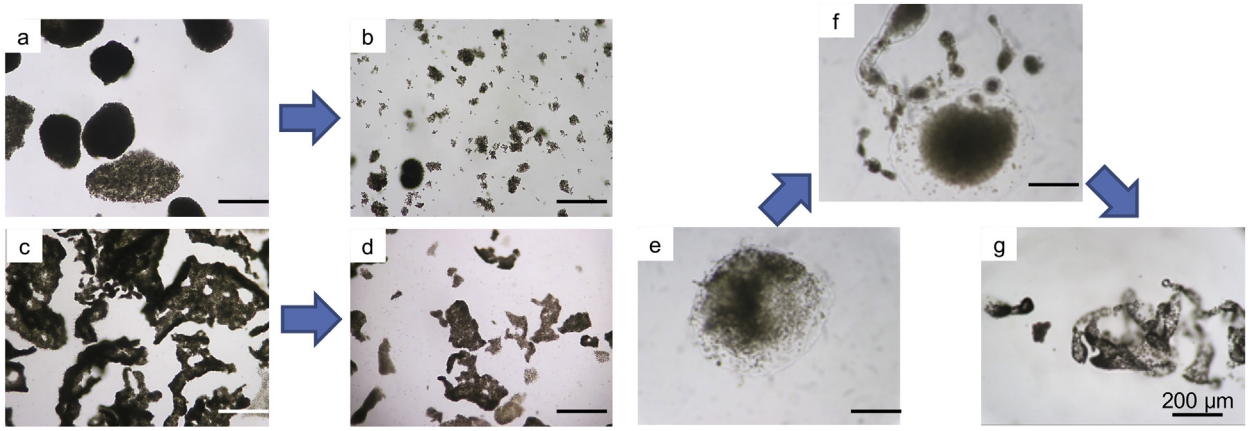

Fig. 4. Photomicrographs of *M. ichthyoblabe*, *M. aeruginosa* and *M. wesenbergii* colonies before and after mixing treatments (a–f). a, initial *M. ichthyoblabe* colonies; b, *M. ichthyoblabe* colonies after 30-min mixing; c, initial *M. aeruginosa* colonies; d, *M. aeruginosa* colonies after 30-min mixing; e, initial spherical *M. wesenbergii*; f, transitional *M. wesenbergii* colonies; and g, reticular *M. wesenbergii* colonies after 30-min mixing. The scale bar was marked for all photomicrographs, as 200 μm.

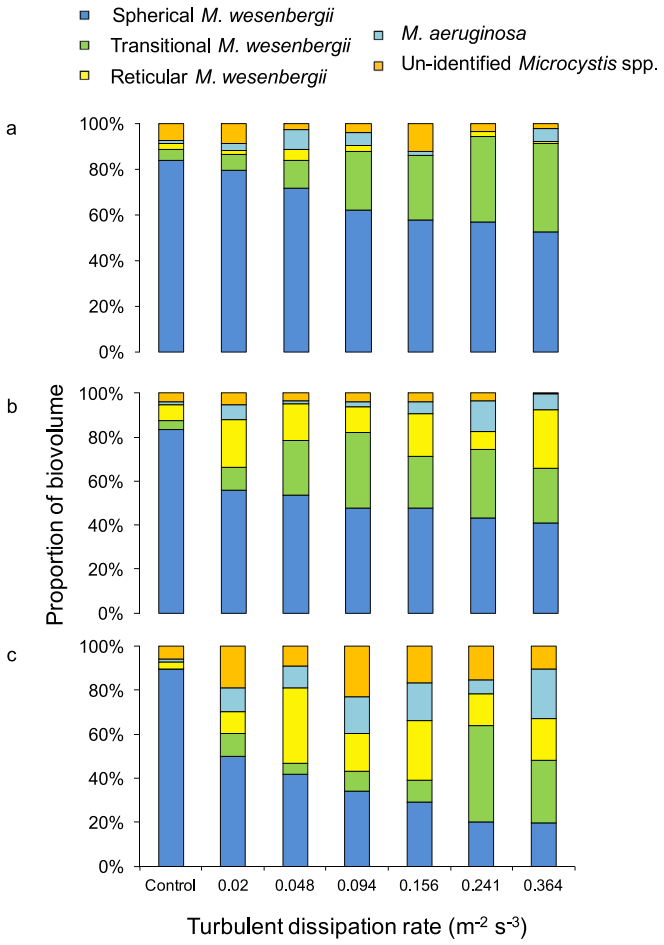

Fig. 5. Volume proportion of colonies in different morphologies before (control) and after the mixing experiments of *M. wesenbergii* colonies under the six turbulent dissipation rates. a – c were the small, medium and large size groups.

blooms in many lentic systems, turbulent dissipation rates in these systems have not been quantified (Visser et al., 2016). Visser et al. (1996) demonstrated successful control of cyanobacterial blooms in Lake Nieuwe Meer (30 m in depth) with an aeration system. They illustrated that the aeration decreased the temperature to <2 °C between the water surface and bottom of the lake. In another 30-m deep lake, Vlietland in the Netherlands, a wind speed of 12 m s^{-1} was found to result in similar levels of density stratification, with *Microcystis* colonies distributed throughout the water depth (Aparicio Medrano et al., 2013). The turbulent dissipation rate of the artificial mixing used in Lake Nieuwe Meer could be deduced from Eq. (1) to be 3.35×10^{-4} m^2 s^{-3}. This dissipation rate is similar to the maximum value reported in Lake Taihu with a wind speed of approximately 4.87 m s^{-1}. Therefore, these artificial mixing devices may potentially partially mix down buoyant surface colonies of *Microcystis* spp. but may not necessarily break up the colonies in a way that occurs with very high dissipation rates occurring in shallow lakes under extreme wind conditions or using our laboratory stirring device.

Laboratory studies have frequently used an oscillating grid and churn-dasher to induce turbulent mixing. The former device has produced mixing with ε in the range 10^{-9} to 10^{-6} m^2 s^{-3} (O'Brien, 2003; Wilkinson et al., 2016), while the later device has generated mixing with ε up to 0.313 m^2 s^{-3} (Hondzo et al., 1997) and 0.080 m^2 s^{-3} (Xiao et al., 2016), respectively. The ε induced in the stirring device of the current study was the same order of magnitude as the values reported in the churn-dasher. Nevertheless, these unrealistic values are not necessarily representative of natural systems.

4.2. Disaggregation of Microcystis colonies by turbulence

Under the artificial mixing rates used in this study, colony disaggregation of *Microcystis* morphospecies was in the order of *M. ichthyoblabe* > *M. aeruginosa* > *M. wesenbergii*. Our order differs from that deduced by Otten and Paerl (2011) because they ranked the spherical colonies, which have tightly arranged cells and no surrounding gelatinous envelope, as hardest to break. These authors categorized the spherical colonies as *M. flos-aquae*, while we considered they were *M. ichthyoblabe*, the easiest to disaggregate under mixing. Consistently, however, *M. wesenbergii* colonies had the highest resistance to turbulence. This is because, unlike *M. ichthyoblabe* and *M. aeruginosa*, *M. wesenbergii* colonies have a clearly distinguishable gelatinous envelope which is composed of pectin-like extracellular polysaccharides (EPSs). Capel et al. (2006) found that during the gelling process of pectin, the shear strength of pectin and pectin-like EPS increased. Thus, the gelatinous envelope encapsulating *M. wesenbergii* colonies appears to be important in conferring resistance to turbulence.

In a previous cyanobacterial mixing experiment by O'Brien et al. (2004) using a grid-stirred tank, the initial D_{50} of *M. aeruginosa* colonies was about 400 μm, which is similar to that of the smallest size group of *M. aeruginosa* in our current study (Fig. 3c). O'Brien et al. (2004) found the maximum stable colony diameter was from 220 to 420 μm, which is also similar to the range of 300–400 μm measured in our experiments after 30 min of mixing. The maximum dissipation rate used by O'Brien et al. (2004) was 9×10^{-5} m^2 s^{-3}, which is however, three orders of magnitude less than our minimum value. One reason for their much lower dissipation rate might be that measurements were outside of the stirred grid where the values are likely to be considerably smaller. *Microcystis* colonies used in our study were collected from large, wind-exposed lakes. The colonies collected from a small, sheltered pond (O'Brien et al., 2004) may be more susceptible and prone to disaggregation with turbulent mixing.

This study showed that colonies of *M. ichthyoblabe* are more fragile than those of *M. aeruginosa* and *M. wesenbergii*. The smallest colony size of *M. ichthyoblabe* was around 40 μm, similar to the Kolmogorov scale, at the highest turbulent dissipation rate of 0.364 m^2 s^{-3}. Therefore, at ε of 0.364 m^2 s^{-3}, *M. ichthyoblabe* colonies had been fully disaggregated to their minimum size and any additional turbulent kinetic energy would be dissipated into heat (Peters and Marrasé, 2000). Mixing with ε of 0.020 m^2 s^{-3}, i.e., four orders of magnitude higher than the largest values measured in deep lakes (Wüest and Lorke, 2003), had little disaggregating effect on *M. ichthyoblabe* colonies. Our results indicate that large colonies are not as fragile as has been postulated (e.g., (Otten and Paerl, 2011)) and colony morphology associated with differences in *Microcystis* morphospecies may be more significant than colony size *per se*.

The impellers in our mixing device may break down the colonies directly. However, Fig. 3a illustrates that the minimum size of disaggregated colonies was similar to the Kolmogorov scale (μm), suggesting that the main disaggregating effect is from the mixing but not directly from the impellers. The decrease in D_{50} of the colonies with time appears to follow an exponential decay, suggesting a first order kinetic reaction. This reaction suggested that the decrease rate of D_{50} was a constant at each dissipation rate.

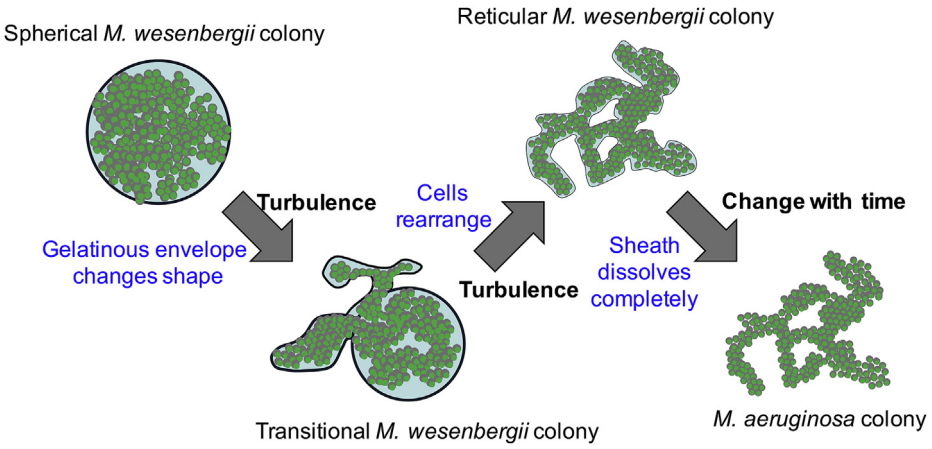

Fig. 6. Conceptual model of morphological changes in *M. wesenbergii*-like colonies to *M. aeruginosa-like* colonies.

4.3. Changes in colony morphology induced by turbulence

Our experiment also illustrated that the tightly packed cells in *M. ichthyoblabe* colonies were easily disaggregated into smaller colonies comprised of loosely bound cells. *M. flos-aquae* has sometimes been recognized as a morphotype of *M. ichthyoblabe*; a taxonomic classification also noted by Watanabe, (1996). Any changes in colony morphology of *M. aeruginosa* exposed to turbulence were not recognizable in the current study.

M. wesenbergii has been found to be morphologically and genetically distinct from other *Microcystis* morphospecies, e.g., *M. aeruginosa*, *M. flos-aquae*, and *M. ichthyoblabe*, based on 16S-23S rDNA-ITS sequences (Otten and Paerl, 2011) or gene *cpc*BA-IGS (Tan et al., 2010). However, Xu et al. (2016) found a contradictory result from the high homozygosity in sequences of 16S-23S and *cpc*BA-IGS in a range of *Microcystis* samples except for one *M. aeruginosa* colony. It appears to be extremely difficult to identify different *Microcystis* morphospecies using molecular tools, such as 16S rDNA (Harke et al., 2016; Otsuka et al., 1998; Xu et al., 2014), 16S-23S rDNA (Otsuka et al., 1999; Xu et al., 2016), genomic DNA homologies (Otsuka et al., 2001) or fatty acid analysis (Le Ai Nguyen et al., 2012). These studies all indicate morphology of *Microcystis* colonies changes under different environmental conditions and that classical taxonomic studies should still be used to complement modern molecular techniques.

Spherical *M. wesenbergii* colonies gradually transformed to reticular *M. wesenbergii*-like colonies and then *M. aeruginosa*-like colonies in our experiment. The reticular *M. wesenbergii* colonies have been identified as *M. aeruginosa* when the distinguishable gelatinous envelope is solubilized with EPS (Otsuka et al., 2000). Li et al. (2014b) suggested that solubilisation of mucilage induces changes in colony morphology resulting in transitions from *M. wesenbergii* to *M. aeruginosa*. A conceptualization of our hypothesis regarding changes in colonial morphology from *M. wesenbergii* to *M. aeruginosa* is shown in Fig. 6. Turbulent mixing induces spherical *M. wesenbergii* colonies to change into reticular *M. wesenbergii*-like colonies, and the further solubilisation of mucilage removes the distinguishable gelatinous envelope, resulting in *M. aeruginosa*-like colonies. The phenomenon of mucilage solubilisation was described previously as a dilution process of polysaccharide in the mucilage with time (Li et al., 2014b; Xiao et al., 2018).

M. wesenbergii has been considered as a unique species in the *Microcystis* genera at both phenotypic and genetic level (Otten and Paerl, 2011). Our results suggest that *Microcystis* can change spontaneously from *M. wesenbergii* colonies into *M. aeruginosa*-like colonies under mixing. This observation might explain the absence of sequence-based differences in morphospecies (Otsuka et al. 1998, 2001, 1999; Tan et al., 2010; Xu et al. 2014, 2016).

4.4. Artificial mixing to control blooms by reducing Microcystis colony size

Reducing colony size of *Microcystis* has been considered as a possible method to prevent occurrence of *Microcystis* blooms (Zhu et al., 2016). Our results showed that artificial mixing significantly reduced colony size of *M. ichthyoblabe* but not that of *M. wesenbergii* or *M. aeruginosa*. In many freshwater systems, such as Lakes Taihu, Chaohu (China), Suwa (Japan) and Biwa (Japan), *M. ichthyoblabe, M. wesenbergii and M. aeruginosa* sequentially dominate from late spring to late autumn (Jia et al., 2011; Ozawa et al., 2005; Park et al., 1993; Yamamoto and Nakahara, 2009; Zhu et al., 2016). This seasonal succession provides a period when *M. ichthyoblabe* dominates phytoplankton biomass and artificial mixing could be applied to disaggregate *M. ichthyoblabe* colonies. Our experiment showed that for a turbulent dissipation rate of 0.364 $m^2 s^{-3}$, D_{50} of *M. ichthyoblabe* colonies was <100 μm after 10 min of mixing and <40 μm after 30 min of mixing. Zhu et al. (2014) suggested that if colony size of *Microcystis* is < 100 μm in Lake Taihu, blooms would not occur as the small colonies would be unable to disentrain from the wind induced mixing. Hence, continuous artificial mixing at dissipation rates of 0.364 $m^2 s^{-3}$ for 10 min could effectively reduce *Microcystis* colony sizes, and may be most effective at a time when *M. ichthyoblabe* dominates.

Artificial mixing has successfully reduced *Microcystis* blooms in several lakes, such as Nieuwe Meer in The Netherlands (Jungo et al., 2001; Visser et al., 1996), Lake Dalbang in South Korea (Heo and Kim, 2004) and Bleioch Reservoir in Germany (Becker et al., 2006). It mixes *Microcystis* colonies to deeper layers and induces greater light limitation. In other cases, however, artificial mixing has failed to control blooms (Jöhnk et al., 2008; Lilndenschmidt, 1999; Tsukada et al., 2006), and this may be related to the morphospecies present, the mixing regime used (continuous mixing or intermittent pulses), and the duration of mixing (Visser et al., 2016). Our study sheds new light on why failures may have occurred and it allows for *a priori* assessment of the design requirements for implementation of an effective artificial mixing system. Besides colony formation, over-buoyancy of colonies also plays an important role in the occurrence of *Microcystis* blooms (Ibelings et al., 1991). The buoyancy of *Microcystis* colonies has been attributed to formation of intra-cellular gas vesicles (Pfeifer, 2012) and intra-colony gas bubbles (Aparicio Medrano et al., 2013). Both gas

vesicles and bubbles may be destroyed physically (Zhang et al., 2006). So far, what governs the actual size of colonies is still unknown. Thus, artificially reducing colony size of *Microcystis* should also be considered in freshwater management, as well as controlling the over-buoyancy of *Microcystis* colonies.

5. Conclusions

This study quantified the morphological change and disaggregation of colonies of three *Microcystis* morphospecies to a range of mixing intensities, and sheds new light on buoyancy and succession of these morphospecies. Disaggregation of *Microcystis* colonies in response to turbulence varied with morphospecies, ranking in the order of *M. ichthyoblabe* > *M. aeruginosa* > *M. wesenbergii*. At laboratory induced dissipation rates >0.094 $m^2 s^{-3}$, *M. ichthyoblabe* colonies disaggregated while *M. wesenbergii* barely changed. The dissipation rates used in the current study are three to four orders of magnitude higher than the measured ranges in deep lakes, however, the very high values are theoretically possible under strong winds or with extremely high rates of artificial mixing. Our mixing experiments portended that wind shear may be expected to have a significant effect only on *M. ichthyoblabe* colonies *in situ*. We also deduced that turbulence induced morphological changes in *Microcystis* colonies related to membrane visibility and porosity of colonies, and membrane integrity should be further investigated under different turbulent regimes using alcian blue dye treatment.

Acknowledgements

This work was supported by the National Natural Science Foundation of China [Grant no. 51409216]; the Scientific Research and Service Platform fund of Henan Province (2016151); the Australian Research Council [ARC: linkage project LP130100311]; and a Griffith University Postgraduate International Scholarship. Dr. Ming Li is funded as Tang Scholar by Cyrus Tang Foundation and Northwest A&F University.

Appendix A. Supplementary data

Supplementary data related to this article can be found at https://doi.org/10.1016/j.watres.2018.05.017.

References

Aparicio Medrano, E., Uittenbogaard, R.E., Dionisio Pires, L.M., van de Wiel, B.J.H., Clercx, H.J.H., 2013. Coupling hydrodynamics and buoyancy regulation in *Microcystis aeruginosa* for its vertical distribution in lakes. Ecol. Model. 248, 41–56.
Becker, A., Herschel, A., Wilhelm, C., 2006. Biological effects of incomplete destratification of hypertrophic freshwater reservoir. Hydrobiologia 559, 85–100.
Capel, F., Nicolai, T., Durand, D., Boulenguer, P., Langendorff, V., 2006. Calcium and acid induced gelation of (amidated) low methoxyl pectin. Food Hydrocolloids 20, 901–907.
Duan, H., Ma, R., Xu, X., Kong, F., Zhang, S., Kong, W., Hao, J., Shang, L., 2009. Two-decade reconstruction of algal blooms in China's Lake Taihu. Environ. Sci. Technol. 43, 3522–3528.
Galindo Torres, S., Scheuermann, A., Ruest, M., 2016. Simulation Engine for Fluid Solid Interaction Problems and its Application to the Modelling of Air Blast Hazards in Block Cave Mining (AGU Fall Meeting Abstracts).
Galindo-Torres, S., 2013. A coupled Discrete Element Lattice Boltzmann Method for the simulation of fluid-solid interaction with particles of general shapes. Comput. Meth. Appl. Mech. Eng. 265, 107–119.
Galindo-Torres, S., Pedroso, D., Williams, D., Li, L., 2012. Breaking processes in three-dimensional bonded granular materials with general shapes. Comput. Phys. Commun. 183, 266–277.
Harke, M.J., Steffen, M.M., Gobler, C.J., Otten, T.G., Wilhelm, S.W., Wood, S.A., Paerl, H.W., 2016. A review of the global ecology, genomics, and biogeography of the toxic cyanobacterium, *Microcystis* spp. Harmful Algae 54, 4–20.
Heo, W.-M., Kim, B., 2004. The effect of artificial destratification on phytoplankton in a reservoir. Hydrobiologia 524, 229–239.
Hondzo, M.M., Kapur, A., Lembi, C.A., 1997. The effect of small-scale fluid motion on the green alga *Scenedesmus quadricauda*. Hydrobiologia 364, 225–235.
Ibelings, B.W., Mur, L.R., Kinsman, R., Walsby, A., 1991. Microcystis changes its buoyancy in response to the average irradiance in the surface mixed layer. Arch. Hydrobiol. 120, 385–401.
Jia, X., Shi, D., Shi, M., Li, R., Song, L., Fang, H., Yu, G., Li, X., Du, G., 2011. Formation of cyanobacterial blooms in Lake Chaohu and the photosynthesis of dominant species hypothesis. Acta Ecol. Sin. 31, 2968–2977.
Jöhnk, K.D., Huisman, J.E.F., Sharples, J., Sommeijer, B.E.N., Visser, P.M., Stroom, J.M., 2008. Summer heatwaves promote blooms of harmful cyanobacteria. Global Change Biol. 14, 495–512.
Jungo, E., Visser, P.M., Stroom, J., Mur, L.R., 2001. Artificial mixing to reduce growth of the blue-green alga *Microcystis* in Lake Nieuwe Meer, Amsterdam: an evaluation of 7 years of experience. Water Sci. Technol. Water Supply 1, 17–23.
Le Ai Nguyen, V., Tanabe, Y., Matsuura, H., Kaya, K., Watanabe, M.M., 2012. Morphological, biochemical and phylogenetic assessments of water-bloom-forming tropical morphospecies of *Microcystis* (Chroococcales, Cyanobacteria). Phycol. Res. 60, 208–222.
Li, M., Zhu, W., Gao, L., 2014a. Analysis of cell concentration, volume concentration, and colony size of *Microcystis* via laser particle analyzer. Environ. Manag. 53, 947–958.
Li, M., Zhu, W., Gao, L., Lu, L., 2013. Changes in extracellular polysaccharide content and morphology of *Microcystis aeruginosa* at different specific growth rates. J. Appl. Phycol. 25, 1023–1030.
Li, M., Zhu, W., Guo, L., Hu, J., Chen, H., Xiao, M., 2016. To increase size or decrease density? Different *Microcystis* species has different choice to form blooms. Sci. Rep. 6, 37056.
Li, M., Zhu, W., Sun, Q., 2014b. Solubilisation of mucilage induces changes in *Microcystis* colonial morphology. New Zeal. J. Mar. Fresh 48, 38–47.
Lilndenschmidt, K.E., 1999. Controlling the growth of *Microcystis* using surged artificial aeration. Int. Rev. Hydrobiol. 84, 243–254.
MacKenzie, B., Leggett, W., 1993. Wind-based models for estimating the dissipation rates of turbulent energy in aquatic environments: empirical comparisons. Mar. Ecol. Prog. Ser. 94, 207–216.
O'Brien, K.R., 2003. The Effects of Turbulent Mixing on the Vertical Distribution and Biomass of Phytoplankton Populations. University of Western Australia.
O'Brien, K.R., Meyer, D.L., Waite, A.M., Ivey, G.N., Hamilton, D.P., 2004. Disaggregation of *Microcystis aeruginosa* colonies under turbulent mixing: laboratory experiments in a grid-stirred tank. Hydrobiologia 519, 143–152.
Oliver, R.L., Hamilton, D.P., Brookes, J.D., Ganf, G.G., 2012. Ecology of Cyanobacteria II. Springer, pp. 155–194.
Otsuka, S., Suda, S., Li, R., Matsumoto, S., Watanabe, M.M., 2000. Morphological variability of colonies of *Microcystis* morphospecies in culture. J. Gen. Appl. Microbiol. 46, 39–50.
Otsuka, S., Suda, S., Li, R., Watanabe, M., Oyaizu, H., Matsumoto, S., Watanabe, M.M., 1998. 16S rDNA sequences and phylogenetic analyses of *Microcystis* strains with and without phycoerythrin. FEMS Microbiol. Lett. 164, 119–124.
Otsuka, S., Suda, S., Li, R., Watanabe, M., Oyaizu, H., Matsumoto, S., Watanabe, M.M., 1999. Phylogenetic relationships between toxic and non-toxic strains of the genus *Microcystis* based on 16S to 23S internal transcribed spacer sequence. FEMS Microbiol. Lett. 172, 15–21.
Otsuka, S., Suda, S., Shibata, S., Oyaizu, H., Matsumoto, S., Watanabe, M.M., 2001. A proposal for the unification of five species of the cyanobacterial genus *Microcystis* Kutzing ex Lemmermann 1907 under the rules of the Bacteriological Code. Int. J. Syst. Evol. Microbiol. 51, 873–879.
Otten, T.G., Paerl, H.W., 2011. Phylogenetic inference of colony isolates comprising seasonal *Microcystis* blooms in Lake Taihu, China. Microb. Ecol. 62, 907–918.
Ozawa, K., Fujioka, H., Muranaka, M., Yokoyama, A., Katagami, Y., Homma, T., Ishikawa, K., Tsujimura, S., Kumagai, M., Watanabe, M.F., Park, H.D., 2005. Spatial distribution and temporal variation of *Microcystis* species composition and microcystin concentration in Lake Biwa. Environ. Toxicol. 20, 270–276.
Park, H.D., Watanabe, M.F., Harada, K.I., Suzuki, M., Hayashi, H., Okino, T., 1993. Seasonal variations of *Microcystis* species and toxic heptapeptide microcystins in Lake Suwa. Environ. Toxicol. Water Qual. 8, 425–435.
Peters, F., Marrasé, C., 2000. Effects of turbulence on plankton: an overview of experimental evidence and some theoretical considerations. Mar. Ecol. Prog. Ser. 205, 291–306.
Pfeifer, F., 2012. Distribution, formation and regulation of gas vesicles. Nat. Rev. Microbiol. 10, 705–715.
Regel, R.H., Brookes, J.D., Ganf, G.G., Griffiths, R.W., 2004. The influence of experimentally generated turbulence on the Mash01 unicellular *Microcystis aeruginosa* strain. Hydrobiologia 517, 107–120.
Rowe, M., Anderson, E., Wynne, T., Stumpf, R., Fanslow, D., Kijanka, K., Vanderploeg, H., Strickler, J., Davis, T., 2016. Vertical distribution of buoyant *Microcystis* blooms in a Lagrangian particle tracking model for short-term forecasts in Lake Erie. J. Geophys. Res. Oceans 121, 5296–5314.
Tan, W., Liu, Y., Wu, Z., Lin, S., Yu, G., Yu, B., Li, R., 2010. cpcBA-IGS as an effective marker to characterize *Microcystis wesenbergii* (Komárek) Komárek in Kondrateva (cyanobacteria). Harmful Algae 9, 607–612.
Tsukada, H., Tsujimura, S., Nakahara, H., 2006. Seasonal succession of phytoplankton in Lake Yogo over 2 years: effect of artificial manipulation. Limnology 7, 3–14.
Visser, P.M., Ibelings, B.W., Bormans, M., Huisman, J., 2016. Artificial mixing to control cyanobacterial blooms: a review. Aquat. Ecol. 50, 423–441.
Visser, P.M., Ibelings, B.W., van der Veer, B., Koedood, J., Mur, L.R., 1996. Artificial mixing prevents nuisance blooms of the cyanobacterium *Microcystis* in Lake

Nieuwe Meer, The Netherlands. Freshw. Biol. 36, 435–450.
Wallace, B.B., Bailey, M.C., Hamilton, D.P., 2000. Simulation of vertical position of buoyancy regulating *Microcystis aeruginosa* in a shallow eutrophic lake. Aquat. Sci. 62, 320–333.
Wang, Z., Wu, T., Zou, H., Jia, X., Huang, L., Liang, C., Zhang, C., 2016. Changes in seasonal characteristics of wind and wave in different regions of Lake Taihu. J. Lake Sci. 28, 217–224 (Chinese with English Abstract).
Watanabe, M., 1996. Isolation, cultivation and classification of bloom-forming *Microcystis* in Japan. Toxic Microcystis 2, 13–34.
Wilkinson, A., Hondzo, M., Guala, M., 2016. Effect of small-scale turbulence on the growth and metabolism of *Microcystis aeruginosa*. Adv. Microbiol. 6, 351–367.
Wüest, A., Lorke, A., 2003. Small-scale hydrodynamics in lakes. Annu. Rev. Fluid Mech. 35, 373–412.
Xiao, M., Li, M., Reynolds, C.S., 2018. Colony formation in the cyanobacterium Microcystis. Biol. Rev. Camb. Phil. Soc. https://doi.org/10.1111/brv.12401.
Xiao, Y., Li, Z., Li, C., Zhang, Z., Guo, J., 2016. Effect of small-scale turbulence on the physiology and morphology of two bloom-forming cyanobacteria. PLoS One 11, e0168925.
Xu, S., Peng, Q., Li, M., 2014. Morphospecies and genospecies of *Microcystis* during blooms in eutrophic Lake Taihu (China) in autumn. Biochem. Systemat. Ecol. 57, 322–327.
Xu, S., Sun, Q., Zhou, X., Tan, X., Xiao, M., Zhu, W., Li, M., 2016. Polysaccharide biosynthesis-related genes explain phenotype-genotype correlation of *Microcystis* colonies in Meiliang Bay of Lake Taihu, China. Sci. Rep. 6, 35551.
Yamamoto, Y., Nakahara, H., 2009. Seasonal variations in the morphology of bloom-forming cyanobacteria in a eutrophic pond. Limnology 10, 185–193.
Yang, Z., Kong, F., Shi, X., Zhang, M., Xing, P., Cao, H., 2008. Changes in the morphology and polysaccharide content of *Microcystis aeruginosa* (Cyanobacteria) during flagellate grazing. J. Phycol. 44, 716–720.
Yu, G., Song, L., Li, R., 2007. Taxonomic notes on water bloom forming *Microcystis species* (Cyanophyta) from China-an example from samples of the Dianchi lake. Acta Phytotaxon. Sin. 45, 727–741 (Chinese with English Abstract).
Zhang, G., Zhang, P., Wang, B., Liu, H., 2006. Ultrasonic frequency effects on the removal of *Microcystis aeruginosa*. Ultrason. Sonochem. 13, 446–450.
Zhang, P., Galindo-Torres, S., Tang, H., Jin, G., Scheuermann, A., Li, L., 2017. An efficient Discrete Element Lattice Boltzmann model for simulation of particle-fluid, particle-particle interactions. Comput. Fluids 147, 63–71.
Zhang, P., Galindo-Torres, S.A., Tang, H., Jin, G., Scheuermann, A., Li, L., 2016. Lattice Boltzmann simulations of settling behaviors of irregularly shaped particles. Phys. Rev. E 93, 062612.
Zhou, J., Qin, B., Han, X., Zhu, L., 2016. Turbulence increases the risk of microcystin exposure in a eutrophic lake (Lake Taihu) during cyanobacterial bloom periods. Harmful Algae 55, 213–220.
Zhu, W., Li, M., Luo, Y., Dai, X., Guo, L., Xiao, M., Huang, J., Tan, X., 2014. Vertical distribution of *Microcystis* colony size in Lake Taihu: its role in algal blooms. J. Great Lake. Res. 40, 949–955.
Zhu, W., Zhou, X., Chen, H., Gao, L., Xiao, M., Li, M., 2016. High nutrient concentration and temperature alleviated formation of large colonies of *Microcystis*: evidence from field investigations and laboratory experiments. Water Res. 101, 167–175.